

Precise B-doped Ultrananocrystalline Diamond Nanowire Arrays for high performance of CO Gas Sensor

Xiaoyan Peng^{a,b*}, Yiming Li^b, Shukai Duan^a, Jin Chu^a, Peter Feng^{b,*}

^a*College of Artificial Intelligent, Southwest University, Chongqing, 400715, China*

^b*Department of Physics, University of Puerto Rico, San Juan, 00931, USA*

* Author to whom correspondence should be addressed. Electronic mail: pengxy_physics@163.com, peter.feng@upr.edu

Abstract: We report that the boron-doped Ultrananocrystalline diamond (UNCD) nanowires with extremely high length to diameter ratio and oxygen functional groups possess an intrinsic nature capable of adsorbing carbon monoxide (CO) molecules. The purpose is to develop high performance of UNCD nanowire arrays gas sensor. Highly flat UNCD thin film with thickness of 70 nm was firstly grown on Si substrate. The film main consists of a large amount of UNCD grain with size smaller than 10 nm. (it sounds 3-4 nm, please check is again) Successive processes were performed afterward to fabricate three groups of UNCD nanowire arrays. Then the sensing performances of the fabricated devices with different structures including serial connection of the nanowires and parallel connection of the nanowires were evaluated. Furthermore, corresponding kinetic model and sensing mechanism have also been discussed. Small grain size, high length to diameter ratio and the existence of oxygen functional groups have been ascribed as the key factors for promoting CO gas adsorption that largely enhances device gas sensitivity.

Keywords: UNCD materials; nanowire arrays, gas sensors;

1. Introduction

Carbon monoxide (CO) is an invisible, odorless but dangerous gas due to its serious toxicity and

flammability. Much impressive research has been accomplished in detection and controlling CO at a low concentration and consequently various types of CO gas sensors have been fabricated. Hyodo [1] and Gupta [2] et al. applied diode-type and optical gas sensors to improve CO response, respectively. Ultrananocrystalline diamond (UNCD) has been heavily explored in recent years mainly due to its chemical inertness, extremely small grain size and high wear/corrosion resistance. Furthermore, the physical, chemical and biological compatibility properties of UNCD can be further modified with either nitrogen incorporated into grain boundaries [3] or boron atoms substituted into diamond lattice [4]. Boron-doped UNCD has found its way into chemical sensor application especially at high temperature or in harsh environments [5] and tiny sensor arrays with nanostructures are desirable when considering the use in micro- and nano- electromechanical systems.

In this work, micrometer-size CO sensing device with diamond nanowire arrays have been fabricated. Field emission scanning electron microscopy (FESEM), atomic force microscopy (AFM) and X-ray photoelectron spectroscopy (XPS) analysis were used to characterize the sample, followed by CO sensing characterizations and mechanism analysis of three groups of nanowires arrays with different connections in order to understand how the length of nanowires effect on the sensing performance.

2. Experimental details

The sample is consisted of three groups of boron-doped UNCD nanowires on an insulating Si substrate with four Au electrodes, creating a sensor array device. Firstly, diamond nanopowders were seeded and boron-doped UNCD thin film was grown via a microwave plasma chemical vapor deposition (MPCVD) process. Trimethylboron gas was injected into the chamber during deposition

to achieve boron doping of the UNCD film. Then four well-arranged Au electrodes were grown abreast in a sputtering system. Electron beam lithography (EBL) patterning and reactive ion etching (RIE) processes were performed afterward to fabricate UNCD nanowires and remove the residual material, followed by an annealing process. The detailed experimental procedures can be found in reference [6]. The as-prepared sample was characterized, cleaned by concentrated sulfuric acid to remove the amorphous carbon, after which the sensor performances were evaluated in a reported home-made system [7].

3. Results and discussions

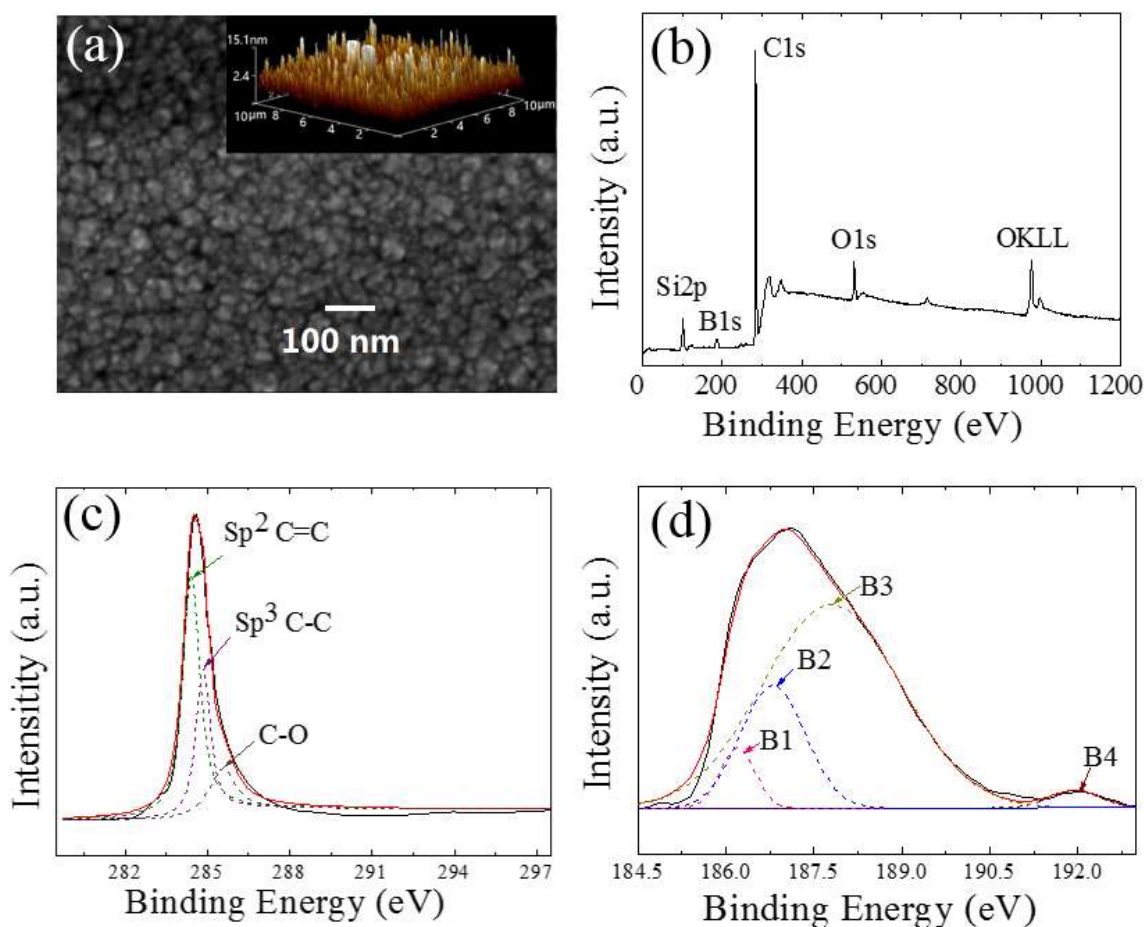


Fig.1 (a) FESEM and AFM images (inset) of the UNCD thin film; (b) XPS survey, and deconvoluted high-resolution (c) C 1s, (d) B 1s spectra of the UNCD thin film.

The FESEM in Fig. 1(a) shows the typical surface morphology of UNCD film with grain size less than 10 nm and the corresponding three-dimensional AFM image was shown as an inset. A root mean square (RMS) roughness of around 5 nm verifies a smooth surface of the UNCD film, which is a prerequisite for subsequent process of highly ordered UNCD nanowires. Diamond seeding process prior to the deposition is essential to enhance the nucleation of diamond grains substrate [8]. XPS analysis was further conducted to determine the elemental compositions of the UNCD thin film. Fig. 1(b) shows a sharp C1s peak near 284.6 eV and a small, but quantifiable, B1s peak at 188 eV. The C1s spectrum presented in Fig. 1(c) is curve-fitted into three peak components with the binding energy of 284 ± 0.5 , 285 ± 0.5 and 286 ± 0.5 eV, which are attributed to sp^2 , sp^3 and C-O bonds, respectively [9]. The existence of oxygen functional groups can work as active sites to promote gas adsorption [10]. The four components of the B1s are denoted as B₁ to B₄, as shown in Fig. 1(d). The peaks at ~ 186.2 and 186.8 eV are attributed to the B-C bond in B₄C and the peak at 187.8 eV is assigned to BC_{3,4} [11], while the bond at 192 eV is attributed to B=O [12].

After characterizations, Au electrodes were deposited on the surface of UNCD thin film and EBL/RIE processes were performed afterward to fabricate UNCD nanowires. The gaps between two adjacent Au electrodes are 5, 10, and $20 \mu\text{m}$, respectively, as shown in Fig. 2(a). The FESEM image in Fig. 2(b) displays a group of the nanowires with the length and diameter of $20 \mu\text{m}$ and 100 nm , respectively. Any endeavor to further increase length to diameter ratio always induces bend and breakage of the nanowires. Each UNCD nanowire is controlled as the same in width and two parallel adjacent nanowires have identical distance, as exhibited in Fig. 2(b). Fig. 2(c) shows the schematic diagram of structure of the sensor arrays with four Au electrodes and three groups of boron-doped UNCD nanowires (denoted by r_1 , r_2 , and r_3). Here, the lengths of r_1 , r_2 and r_3 are in accordance with

the gaps between Au electrodes as 5, 10 and 20 μm , respectively. Four electrodes can be chosen to connect with an AC ($V_0 = 1\text{V}$, 1000 Hz) power supply and a precise resistor to form electrical circuits to realize the serial connected nanowires (SCNs) and paralleled connected nanowires (PCNs) structure. One of the advantages of the present sensor arrays is that each group of nanowires can be directly connected to external electrical circuits by altering electrodes to poles, as described in the caption of Fig. 2(d) and 2(e).

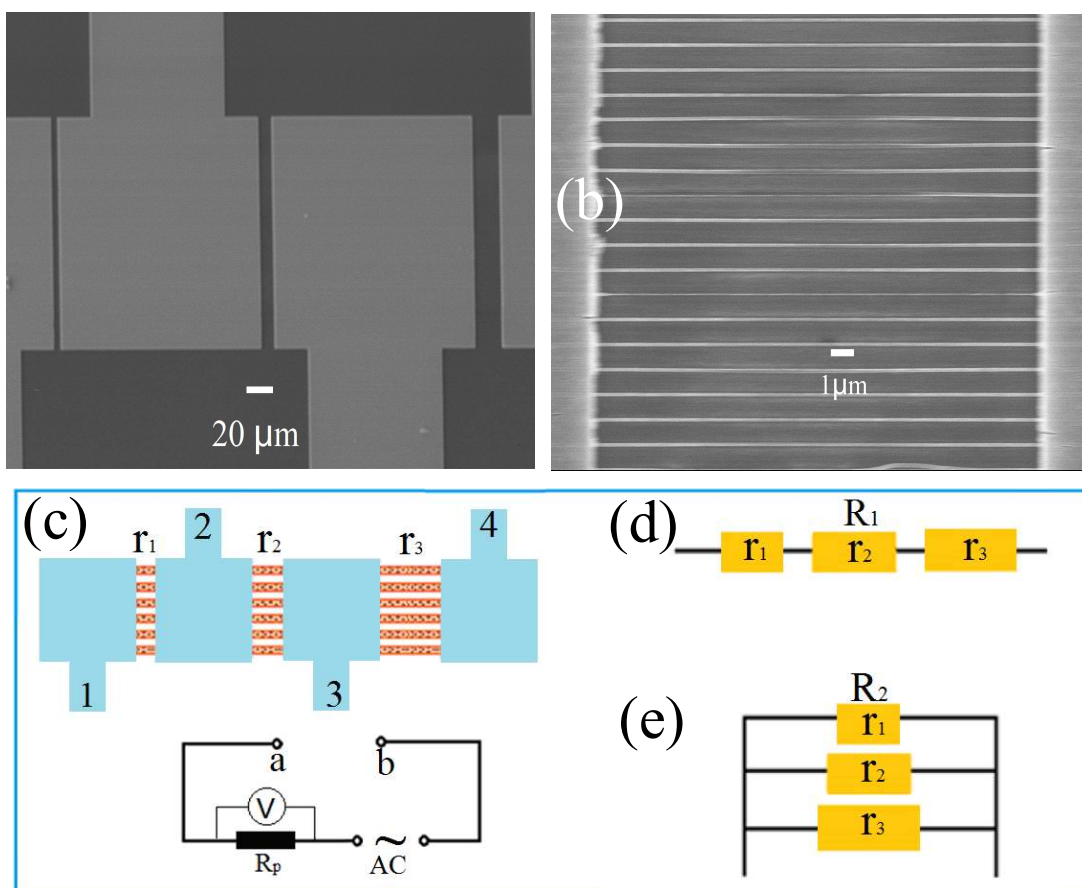


Fig. 2 (a) FESEM image of Au electrodes; (b) Enlarged FESEM image of the UNCD with lengths of 20 μm ; (c) Schematic diagram of the sensor array structure with four electrodes (labeled as 1, 2, 3, and 4, respectively) layered over UNCD nanowires, and the two poles of power supply, a and b; (d) The equivalent SCNs when connecting 1 to a, and 4 to b, respectively; (e) The equivalent PCNs when connecting 1 and 3 to a, and meanwhile 2 and 4 to b, respectively.

The comparison of transient response of PCNs and r_1 under 50 ppm CO and 200 $^{\circ}\text{C}$ is shown in Fig. 3(a). The response value was defined by $(Z_o - Z_g)/Z_o \times 100\%$, where Z_o and Z_g refer to the

impedance of UNCD at pure air and CO/air mixture gas, respectively. The ambient gas was switched between CO/air mixture gas and pure air for every 50 s. It's clearly visible that PCNs have higher response than r_1 . Fig. 3(b) demonstrates the responses of all the sensors exposed to 50 ppm CO gas ambient, from which it can be easily found that the responses increase with operating temperature. At the same operating temperature, the response strengths of devices increase with their nanowires lengths. As a result, the SCNs and PCNs sensors show higher responses.

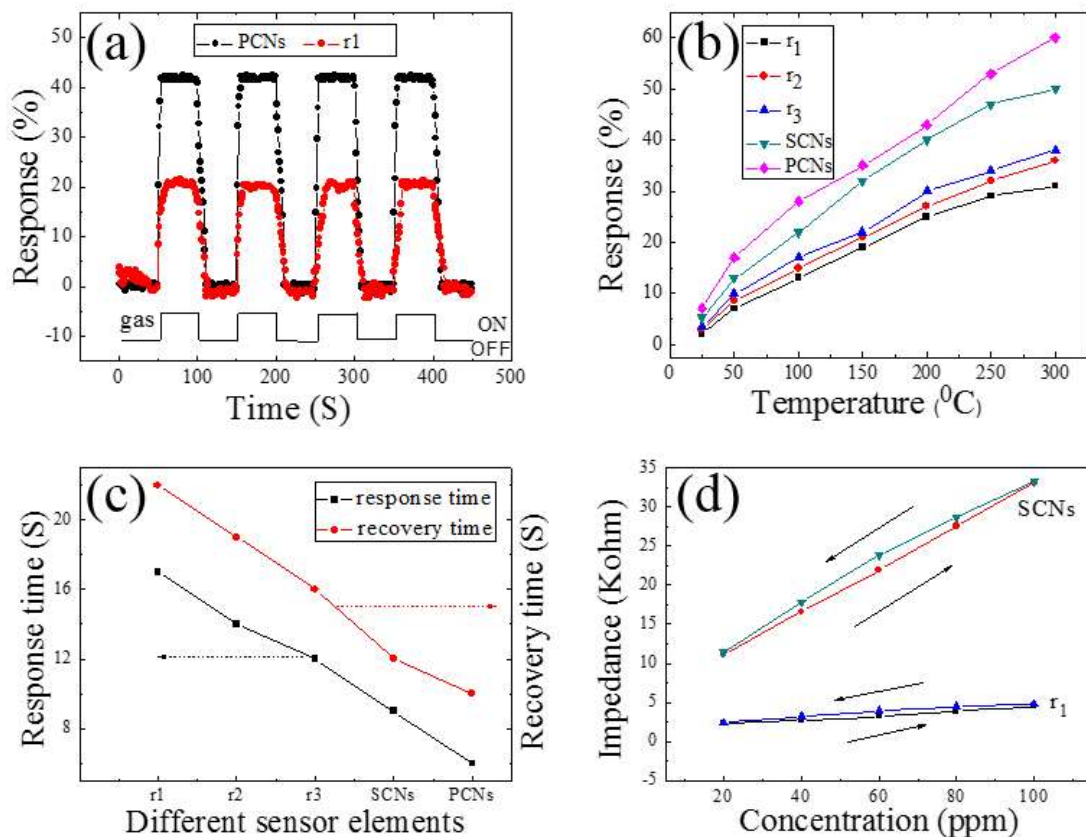


Fig.3 (a) Transient response curves of r_1 and PCNs under 50 ppm CO gas ambient and 200°C; (b) Comparative values of the response; (c) Response and recovery times of all the sensors as a function of operating temperature at 50 ppm CO gas ambient; (d) Absorption-desorption behavior of SCNs and r_1 under different CO concentrations.

Fig. 3(c) indicates the SCNs and PCNs' response and recovery behavior are faster than that of the separated nanowires based devices. The impedance hysteresis characteristics of SCNs and r_1

were exhibited in Fig. 3(d). As seen that the impedance of SCNs increases almost three times, whereas r_1 has only slight change with a variation of CO concentration from 20 to 100 ppm.

It is well known that the O_2 in air will react on conductive surface, and then dissociate into O_2^- , O^- , and O^{2-} when the sensor was exposed to air [13]. When the UNCD with small grain size and large grain boundary was exposed to the target gas, the CO molecules with electron-donating ability also got adsorbed onto the conductive diamond surface. The interaction between the CO and oxygen anions released electrons via the oxidation reactions [6]. This process consequently decreased the total number of the charge carriers of the p-type boron-doped UNCD nanowires by the recombination of the electrons and holes, and led to a decrease in conductivity. For other carbon nanomaterials, such as, graphene [10] and carbon nanotubes [14], charge transfer would be the main proposed sensing mechanism, whereas for transition metal dichalcogenide layers, sensing principle may be related to the variation in effective bandgap and enhancement of the leakage current [15].

4. Conclusions

Three groups of well-arranged boron-doped UNCD nanowires with precise surface and extremely small grain size were controllably fabricated on a Si substrate by using MPCVD, EBL and RIE processes technologies. XPS spectra show boron doping was successfully achieved and the oxygen functional groups were existed in the UNCD.

The present fabricated structures enable the evaluating of the CO sensing properties of separated nanowires groups, SCNs and PCNs based sensor arrays.

All the separated groups of nanowires based sensing devices have high response to CO gas because the small grain size of UNCD and oxygen functional groups provide sites for adsorption of

CO molecules. The obtained experimental data indicated that the newly designed and fabricated sensor arrays can be benefit not only for the utilization of the sensors to integrated circuit, but also for the study for the length-dependence characteristic of the sensing devices.

Acknowledgement

The work was supported by Fundamental Research Funds for the Central Universities (Grant No. XDJK2018C024), Fundamental Science and Advanced Technology Research Foundation of Chongqing (cstc2018jcyjA0870), and NSF-CREST Center for Innovation, Research and Education in Environmental Nanotechnology (CIRE2N) Grant Number HRD-1736093, as well as China Postdoctoral Science Foundation (2017M610582), and Chongqing Postdoctoral Science Foundation (xm2016118).

References

- [1] T. Hyodo, N. Morinaga, Y. Shimizu, *Chemosensors* 6 (2018) 7 (12 pp).
- [2] A. Paliwal, A. Sharma, M. Tomar, V. Gupta, *Sens. Actuators. B: Chem.* 250 (2017) 679–685.
- [3] S. Bhattacharyya et al., *Appl. Phys. Lett.* 79 (2001) 1441–1443.
- [4] M. D. Jaeger, S. Hyun, A. R. Day, M. F. Thorpe, B. Golding, *Appl. Phys. Lett.* 72 (1998) 2445–2447.
- [5] P. Feng, X. P. Wang, A. Aldalbahi, A. F. Zhou, *Appl. Phys. Lett.* 107 (2015) 233103 (4 pp).
- [6] X. Y. Peng, J. Chu, L.D. Wang, S.K. Duan, P. Feng, *Sens. Actuators. B: Chem.* 241 (2017) 383–389.
- [7] X. Y. Peng, S. Muhammad, J. Chu, B. Q. Yang, P. Feng, *Appl. Surf. Sci.* 257 (2011) 4795–4800.
- [8] K. F. Liu, L. J. Chen, N. H. Tai, I. N. Lin, *Diamond Relat. Mater.* 18 (2009) 181–185.
- [9] S. Sotoma et al., *RSC Adv.* 5 (2015)13818–13827.
- [10] W. Jin et al., *Adv. Funct. Mater.* 26 (2016) 7462–7469.
- [11] B. N. Mavrin, et al., *Phys. Lett. A* 372 (2008) 3914–3918.
- [12] A. Prakash, K. B. Sundaram, *Appl. Surf. Sci.* 396 (2017) 484–491.
- [13] M. Takata, D. Tsubone, H. Yanagida, *J. Am. Ceram. Soc.* 59 (1976) 4–8.
- [14] Z. Zanolli, et al., *ACS nano.* 5 (2011) 4592–4599.
- [15] Q. Yue, Z. Shao, S. Chang, J. Li, *Nanoscale Res. Lett.* 8 (2013) 425 (12 pp).
- [16] J. Baek, et al., *Nano Res.* 10 (2017) 1861–1871.